HEPATOLOGY

HEPATOLOGY, VOL. 74, NO. 6, 2021

Modeling PNPLA3-Associated NAFLD Using Human-Induced Pluripotent Stem Cells

Samantha G. Tilson [1-3], Carola M. Morell,[2] An-Sofie Lenaerts,[2] Seung Bum Park,[3] Zongyi Hu,[3] Benjamin Jenkins,[4] Albert Koulman [4], T. Jake Liang [3*] and Ludovic Vallier[2**]

SEE EDITORIAL ON PAGE 2942

BACKGROUND AND AIMS: NAFLD is a growing public health burden. However, the pathogenesis of NAFLD has not yet been fully elucidated, and the importance of genetic factors has only recently been appreciated. Genomic studies have revealed a strong association between NAFLD progression and the I148M variant in patatin-like phospholipase domain-containing protein 3 (PNPLA3). Nonetheless, very little is known about the mechanisms by which this gene and its variants can influence disease development. To investigate these mechanisms, we have developed an *in vitro* model that takes advantage of the unique properties of human-induced pluripotent stem cells (hiPSCs) and the CRISPR/CAS9 gene editing technology.

APPROACH AND RESULTS: We used isogenic hiPSC lines with either a knockout ($PNPLA3^{KO}$) of the PNPLA3 gene or with the I148M variant ($PNPLA3^{I148M}$) to model PNPLA3-associated NAFLD. The resulting hiPSCs were differentiated into hepatocytes, treated with either unsaturated or saturated free fatty acids to induce NAFLD-like phenotypes, and characterized by various functional, transcriptomic, and lipidomic assays. $PNPLA3^{KO}$ hepatocytes showed higher lipid accumulation as well as an altered pattern of response to lipid-induced stress. Interestingly, loss of PNPLA3 also caused a reduction in xenobiotic metabolism and predisposed $PNPLA3^{KO}$ cells to be more susceptible to ethanol-induced and methotrexate-induced toxicity. The $PNPLA3^{I148M}$ cells exhibited an intermediate phenotype between the wild-type and $PNPLA3^{KO}$ cells.

CONCLUSIONS: Together, these results indicate that the I148M variant induces a loss of function predisposing to steatosis and increased susceptibility to hepatotoxins. (Hepatology 2021;74:2998-3017).

NAFLD is now the leading cause of chronic liver disease in the developed world.[(1)] NAFLD is defined by accumulation of fat within the liver, which ranges from simple steatosis to NASH, cirrhosis, and HCC. With approximately one in four adults suffering from some form of the disease, it represents

Abbreviations: A1AT, alpha-1-anti-trypsin; ALB, albumin; BIP, binding immunoglobulin protein; CHOP, C/EBP homologous protein; DNL, de novo lipogenesis; FFA, free fatty acid; hiPSC, human-induced pluripotent stem cell; HL, human liver; HLC, hepatocyte-like cell; HNF4a, hepatocyte nuclear factor 4 alpha; KO, knockout; OA, oleic acid; PA, palmitic acid; PCA, principle component analysis; PHH, primary human hepatocyte; PNPLA3, patatin-like phospholipase domain-containing protein 3; PUFA, polyunsaturated fatty acid; sgRNA, single-guide; SA, stearic acid; SFA, saturated fatty acid; TG, triglyceride; TTR, transthyretin.

Received October 22, 2020; accepted July 6, 2021.

Additional Supporting Information may be found at onlinelibrary.wiley.com/doi/10.1002/hep.32063/suppinfo.

**Senior author.*

***Lead contact.*

Supported by the Intramural Research Program of the National Institute of Diabetes and Digestive and Kidney Diseases (National Institutes of Health [NIH]) and the NIH Oxford Cambridge Scholars Program (T.J.L. and S.G.T.); European Research Council Grant New-Chol (L.V. and S.G.T.), Cambridge Hospitals National Institute for Health Research Biomedical Research Center (L.V. and A.L.); Wellcome Sanger Institute (S.G.T.); NC3Rs project grant and training fellowship (C.M.M.); and the Wellcome Trust and Medical Research Council to the Wellcome Trust–Medical Research Council Cambridge Stem Cell Institute.

© 2021 The Authors. Hepatology published by Wiley Periodicals LLC on behalf of American Association for the Study of Liver Diseases. This is an open access article under the terms of the Creative Commons Attribution-NonCommercial License, which permits use, distribution and reproduction in any medium, provided the original work is properly cited and is not used for commercial purposes.

View this article online at wileyonlinelibrary.com.

DOI 10.1002/hep.32063

Potential conflict of interest: Dr. Vallier consults, owns stock, and holds intellectual property rights with DefiniGEN.

a growing cause of liver-related morbidity and mortality.[2] Despite this growing public health burden, the full pathophysiology of NAFLD remains unclear.

Until recently, NAFLD was considered to be a consequence of metabolic syndrome; however, recent studies suggest that genetic factors influence disease onset and progression.[3] Genome-wide association studies identified the I148M variant of patatin-like phospholipase domain-containing protein 3 (PNPLA3) to be associated with the development and progression of NAFLD, regardless of underlying metabolic disease.[4,5] Since this variant was identified, clinical studies have confirmed the association of this variant with the full spectrum of the disease.[6,7] Studies have shown that this protein could have triglyceride lipase, acyl transferase, and retinyl palmitate hydrolase activity.[8-10] However, the function of PNPLA3 has yet to be fully elucidated. Accordingly, it remains unclear whether the I148M variant is a loss or gain of function variant. *In vitro* studies showed that the I148M variant restricts access of the substrate to the active site of the enzyme and results in a profound loss of lipase activity indicating a possible loss of function.[11] However, when the PNPLA3 protein was knocked out in mice, no phenotype was observed.[12]

This lack of information regarding the functions and disease associations of PNPLA3 could also be explained by species divergence between human and mouse. Indeed, these animal models display two major differences: (1) the mouse and human proteins only share approximately 58% homology, and (2) the mouse protein is highly expressed in adipose tissue while the human protein is expressed 10 times higher in the liver.[9,13,14] Furthermore, when the human PNPLA3 protein is overexpressed in mouse livers, it cannot be nutritionally regulated, indicating that the protein may have distinct functions in each species.[14]

For these reasons, we have chosen to develop an *in vitro* human model of PNPLA3-induced NAFLD. We used CRISPR/CAS9 to generate hiPSC lines with either a complete knockout (KO) of the PNPLA3 gene ($PNPLA3^{KO}$) or with the I148M variant knocked in ($PNPLA3^{I148M}$). The hiPSC lines were then differentiated into hepatocyte-like cells (HLCs) and treated with either oleic acid (OA) or palmitic acid (PA) to induce steatosis and lipotoxicity, respectively. Our data suggest that lack of PNPLA3 expression impairs lipid metabolism, contributing to increased steatosis. The I148M variant was also determined to be a loss of function variant, because $PNPLA3^{I148M}$ cells behaved quite similarly to $PNPLA3^{KO}$ cells. Loss of PNPLA3 functionality resulted in global metabolic dysfunction, leading to increased steatosis and reduced xenobiotic metabolism, which makes cells more susceptible to other forms of hepatotoxicity.

Experimental Procedures

HIPSC CULTURE

The hiPSC lines, FSPS13B[15] and A1ATDR/R,[16] were obtained from the hiPSC Core Facility, Cambridge Biomedical Research Center. The cells were maintained on vitronectin-coated plates in Essential 8 medium at 37°C and 5% CO_2 and split every 5-7 days using 0.5 mM EDTA.

ARTICLE INFORMATION:

From the [1]Wellcome Sanger Institute, Hinxton, United Kingdom; [2]Wellcome Medical Research Council Cambridge Stem Cell Institute, University of Cambridge, Cambridge, United Kingdom; [3]Liver Diseases Branch, National Institute of Diabetes and Digestive and Kidney Diseases, National Institutes of Health, Bethesda, MD; [4]Wellcome Medical Research Council Institute of Metabolic Science, University of Cambridge, Cambridge, United Kingdom.

ADDRESS CORRESPONDENCE AND REPRINT REQUESTS TO:

Ludovic Vallier, Ph.D., F.Med.Sci.
Wellcome Medical Research Council Cambridge Stem Cell Institute
Jeffrey Cheah Biomedical Center, Biomedical Campus
Puddicombe Way
Cambridge CB2 0AW, United Kingdom
E-mail: lv225@cam.ac.uk
Tel.: +44-01223-747475
or

T. Jake Liang, M.D.
Liver Diseases Branch
National Institute of Diabetes and Digestive and Kidney Diseases, National Institutes of Health
BG 10 RM 9B16
10 Center Drive
Bethesda, MD, 20814
E-mail: jake.liang@nih.gov
Tel.: +1-301-496-1721

CRISPR/CAS9 TARGETING

The single-guide RNA (sgRNA) sequences were designed to target exon 3. The sgRNA was cloned into the pX459 expression vector and nucleofected into hiPSCs using the Lonza nucleofection kit. Selection was performed for 48 hours using 1 μg/mL of Puromycin. DNA from selected clonal colonies was extracted, amplified, and purified before sequencing. The sequences for the sgRNA, single-stranded donor oligonucleotides (ssODNs), and genotyping primers can be found in Supporting Table S1.

DIFFERENTIATION PROTOCOL

The differentiation protocol to generate HLCs from hiPSCs was adapted from Hannan et.al.[17] hiPSCs were split into single-cell suspension and seeded at a concentration of 50,000 cells/cm^2 on gelatin-coated plates. Cells were allowed to recover for 48 hours before beginning the differentiation. Throughout differentiation, cells were cultured at 37°C, 5% CO_2, and 5% O_2. A full description of HLC generation and a list of media and supplementation components can be found in Supporting Table S2.

3D CELL CULTURE AND LIPID TREATMENT

For 3D culture experiments, HLCs were dissociated into small clumps with Cell Dissociation Buffer (ThermoFisher Scientific, Waltham, MA) at day 23 of differentiation. Cell count was estimated using the Luna Automated Cell Counter (Logos Biosystems, Annandale, VA). Cells were then resuspended at 2.0×10^6 cells/mL in Growth Factor Reduced Matrigel (Corning, Corning, NY). The Matrigel was dispersed in 24-well plates at 50 μL/well, and the plates were stored upside-down at 37°C until the Matrigel had completely solidified. The Matrigel was then overlaid for 24 hours with 3D culture medium supplemented with 20 ng/mL oncostatin M, and 50 ng/mL HGF.

OA, PA, and stearic acid (SA) were reconstituted to 100 mM in 95% ethanol. A total of 250 μM of each fatty acid was conjugated to 12.5% bovine serum albumin (60°C for 10 minutes) to facilitate uptake into the cells. The cells were maintained in their respective medium for 7 days at 37°C, 5% CO_2, and 5% O_2, with medium changes every 48 hours.

IMMUNOFLUORESCENCE MICROSCOPY, FLOW CYTOMETRY, QUANTITATIVE PCR, LIPIDOMICS, RNA SEQUENCING, AND STATISTICS

See Supporting Materials and Methods for details.

TRIGLYCERIDE BLOCKING ASSAY

Triglyceride formation was blocked using 0.5 μM Triacsin C or 10 μM T863. See Supporting Materials and Methods for details.

TOXICITY ASSAYS

Toxicity was induced in FFA laden cells by treating cells with either 100 mM ethanol for 48 hours followed by 24 hour treatment with 20 ng/mL TNFa or 100μM methotrexate for 7 days. See supporting Materials and Methods for details.

CYTOCHROME P450 ACTIVITY, PRESTO BLUE VIABILITY ASSAY, CASPASE 1 INFLAMMASOME ASSAY

CYP3A4 activity was measured using the P450-Glo CYP3A4 Assay System (Promega, Madison, WI) according to the manufacturer's protocol. Cell viability was measured using the Presto Blue Viability Reagent (ThermoFisher Scientific, Waltham, MA) Caspase 1 activation was measured using the Caspase-Glo 1 Inflammasome Assay System (Promega, Madison, WI). See supporting Materials and Methods for details.

QPCR

Total RNA was extracted using the RNEasy Micro Kit (Qiagen, Germantown, MD) and reverse transcribed using Superscript II Reverse Transcriptase (ThermoFisher Scientific, Waltham, MA). The qPCR master mix was prepared using Kapa Sybr Fast (Kapa Biosystems, Inc., Wilmington, MA). See supporting Materials and Methods for primer sequences and further details.

IMMUNOFLUORESCENCE MICROSCOPY

Cells were fixed using 4% paraformaldehyde and stained with the appropriate primary and secondary antibodies. See supporting Materials and Methods for a detailed protocol and a list of antibodies used.

FLOW CYTOMETRY

HLCs grown in 2D were dissocited using TryplE Express (ThermoFisher Scientific, Waltham, MA), fixed in 4% paraformaldehyde, and stained with 1 μg Bodipy (ThermoFisher Scientific, Waltham, MA) before being analysed by flow cytometry. See supporting Materials and Methods for details.

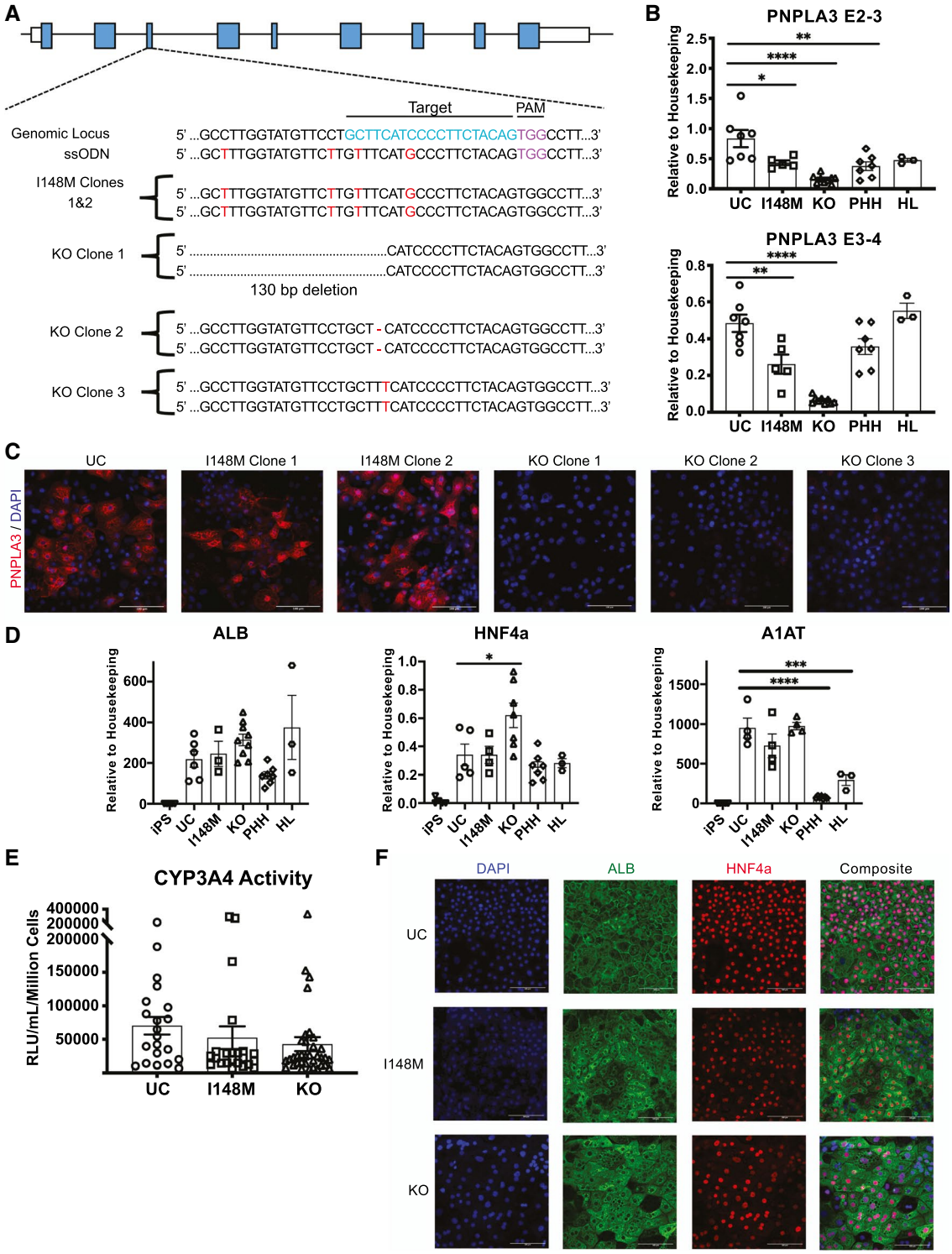

FIG. 1. Editing PNPLA3 does not affect hepatic differentiation capacity. (A) CRISPR/CAS9 targeting strategy at exon 3 of the PNPLA3 gene locus and resulting sequences for the $PNPLA3^{I148M}$ and $PNPLA3^{KO}$ clones used in further experiments. (B) PNPLA3 mRNA expression in HLCs of each genotype at the exon-exon junctions of exons 2 and 3 as well as exons 3 and 4 ($PNPLA3^{UC}$, n = 2 clones and 5 independent experiments; $PNPLA3^{I148M}$, n = 2 clones and 4 independent experiments; $PNPLA3^{KO}$, n = 3 clones and 3 independent experiments) compared with the expression in PHHs (n = 7) and HL samples (n = 3). Ordinary one-way ANOVA with Dunnett's multiple comparisons tests were performed to test statistical significance between means. Data are represented as mean ± SEM. $PNPLA3^{UC}$ cells express high levels of PNPLA3 mRNA, comparable to the expression of PNPLA3 in PHH and HL. $PNPLA3^{KO}$ cells expressed near zero levels of PNPLA3 mRNA. $PNPLA3^{I148M}$ cells expressed high mRNA levels, though slightly lower than those of the $PNPLA3^{UC}$ cells. (C) Protein expression of PNPLA3 following differentiation to HLCs. Expectedly, $PNPLA3^{UC}$ and $PNPLA3^{I148M}$ cells expressed high levels of PNPLA3 protein, while $PNPLA3^{KO}$ cells did not express any detectable levels of PNPLA3 protein. These results indicate that a full knockout of PNPLA3 was achieved in these cells. (D) mRNA expression of hepatocyte functionality markers ALB, HNF4a, and A1AT following hepatocyte differentiation compared with undifferentiated hiPSCs, PHHs, and HLs ($PNPLA3^{UC}$, n = 2 clones and 4 independent experiments; $PNPLA3^{I148M}$, n = 2 clones and 3 independent experiments; $PNPLA3^{KO}$, n = 3 clones and 3 independent experiments; and PHH, n = 7; HL: n = 3). Ordinary one-way ANOVAs with Dunnett's multiple comparisons tests were performed to test statistical significance between means. Data are represented as mean ± SEM. Expression of the three hepatocyte markers is up-regulated from hiPSCs to HLCs, and the expression levels of each gene in the HLCs is similar to or higher than the expression level in PHH and HL, indicating a successful differentiation toward the hepatocyte lineage. Levels of mRNA expression for each marker are similar among the three genotypes, indicating that all genotypes possess a similar capacity to differentiate into HLCs. (E) Basal CYP3A4 activity in HLCs of each genotype was not statistically different, indicating that all genotypes differentiate into HLCs with similar functionality and metabolic activity ($PNPLA3^{UC}$, n = 2 clones and 11 independent experiments; $PNPLA3^{I148M}$, n = 2 clones and 15 independent experiments; and $PNPLA3^{KO}$, n = 3 clones and 15 independent experiments). Ordinary one-way ANOVA with Dunnett's multiple comparisons tests were performed to test statistical significance between means. Data are represented as mean ± SEM. (F) Representative images of ALB and HNF4a protein staining in differentiated cells shows similar expression of mature hepatocyte markers among all three genotypes. See also Supporting Figs. S1-S3.

LIPIDOMICS

Cells were removed from Matrigel using Cell Recovery Solution (Corning, Corning, NY) and the total lipids were extracted using a Folch lipid extraction. The lipids were analysed via direct injection liquid chromatography mass spectromety. The lipidomic data was then analyzed using the MetaboAnalyst web-based analytical pipeline. See supporting Materials and Methods for details.

RNA SEQUENCING

Total RNA was extracted using the RNeasy Micro Kit and the library preparation was performed using the NEBNext Ultra II Directional RNA Library Prep Kit for Illumina (New England BioLabs, Ipswich, MA) according to the manufacturer's protocol. 50 base pair sequencing was performed on the HiSeq 2500 (Illumina, San Diego, CA). See supporting Materials and Methods for details on how data analysis was performed.

STATISTICS

All graphical values are shown as mean ± standard error. Statistical analyses were performed using GraphPad Prism 8 and the R statistical environment. Ordinary one-way ANOVAs with Dunnett's multiple comparisons tests or two-way ANOVAs with Turkey's multiple comparisons tests were performed to test statistical significance between means. P-values less than 0.05 were considered statistically significant.

Results

KNOCKOUT OF PNPLA3 DOES NOT AFFECT HEPATIC DIFFERENTIATION *IN VITRO*

To further understand the function of PNPLA3 in NAFLD pathogenesis, we decided to take advantage of HLCs generated from hiPSCs. This method has been used previously to model a diversity of liver diseases *in vitro*.[18,19] To examine the effect of PNPLA3 genotype on hepatocyte metabolism, we chose to use CRISPR/CAS9 to either knock out PNPLA3 or knock in the I148M variant in two wild-type hiPSC lines with high capacity for hepatocyte differentiation (FSPS13B[15] and A1ATDR/R[16]). This approach allowed for the robust phenotypic comparison of isogenic hiPSC lines while avoiding variability in capacity of differentiation.[20] In sum, off-target optimized sgRNAs targeting exon 3 and ssODN (Fig. 1A

and Supporting Table S2) containing the I148M variant were nucleofected into hiPSCs, and targeted cells were selected using puromycin. Following genotyping and sequencing (Fig. 1A and Supporting Figs. S1-S3), seven FSPS13B sublines (two untargeted control [PNPLA3^{UC}], two variant [PNPLA3^{I148M}], and three KO [PNPLA3^{KO}]) and five A1ATDR/R sublines (two PNPLA3^{UC}, one PNPLA3^{I148M}, and two PNPLA3^{KO}) were chosen for further characterization. Of note, PNPLA3^{UC} lines underwent CRISPR/Cas9 targeting and subcloning but their genetic sequence remained unchanged.

The selected cell lines were then differentiated into HLCs using our established protocol[17] to characterize the expression of PNPLA3 at both the mRNA and protein level (Fig. 1B,C). HLCs derived from PNPLA3^{UC} hiPSCs expressed similar, if not higher, levels of PNPLA3 mRNA when compared with primary human hepatocytes (PHHs) and whole human liver (HL) samples. This high level of PNPLA3 expression was confirmed at the protein level by immunostaining, thereby confirming the utility of these cells to study PNPLA3 function. On the other hand, PNPLA3^{KO} HLCs display extremely low level of PNPLA3 mRNA and undetectable levels of PNPLA3 protein. Notably, PNPLA3^{I148M} HLCs have slightly lower mRNA levels than PNPLA3^{UC} HLCs; however, the expression of PNPLA3 mRNA in PNPLA3^{I148M} HLCs is similar to that of PHHs. Despite the lower mRNA expression in these cells, we found similar levels of PNPLA3 protein in PNPLA3^{I148M} and PNPLA3^{UC} HLCs. Of note, we assessed the effect of insulin and free fatty acid supplementation, two potential inducers of PNPLA3, on the expression of PNPLA3 mRNA[21] and found that expression is not significantly altered by either treatment (Supporting Fig. S4).

We then decided to further characterize HLCs to confirm that changes in PNPLA3 expression and/or CRISPR/CAS9 gene editing did not affect their differentiation and/or function. Gene-expression analyses showed that several key hepatocyte markers including albumin (ALB), hepatocyte nuclear factor 4a (HNF4a), and alpha-1-anti-trypsin (A1AT) maintained similar expression across all genotypes following differentiation (Fig. 1D). The expression of these markers was similar (ALB and HNF4a) or higher (A1AT) in our HLCs compared with PHHs and HLs, indicating that these cells are comparable to primary human samples. Additionally, CYP3A4 activities were comparable among all three genotypes (Fig. 1E), while protein expression of functional hepatocyte markers (ALB and HNF4a) was again similar among the three genotypes (Fig. 1F). Characterization of the A1ATDR/R sublines showed similar results (Supporting Fig. S2). Taken together, these data indicate that all selected hiPSC sublines, regardless of PNPLA3 genotype, can differentiate into HLCs.

PNPLA3 KO AND THE I148M VARIANT PROTECT HLCS AGAINST FATTY ACID–INDUCED STRESS

NAFLD is a complex metabolic disorder that is characterized, in part, by an increased flux of free fatty acids (FFAs) into the liver.[22] After entering the hepatocytes, FFAs can either be stored as metabolically inert triglycerides (TGs) in lipid droplets or metabolized for energy through a variety of pathways including β-oxidation. Overactivity of the β-oxidation pathway can result in the buildup of toxic metabolites and activation of the unfolded protein response, which leads to lipotoxicity.[23] Thus, we decided to analyze the effects of PNPLA3 mutations on steatosis and lipid-induced stress by treating HLCs with OA or PA, respectively. Following a 1-week treatment, lipid accumulation was measured using immunofluorescence or flow cytometry (Fig. 2). In all three treatment groups (control, OA, and PA), PNPLA3^{UC} HLCs accumulated the fewest lipid droplets, PNPLA3^{KO} cells accumulated the most lipid droplets, and the PNPLA3^{I148M} cells exhibited an intermediate phenotype between the two. These differences were most profound in the PA-treated group, in which only 40% of PNPLA3^{UC} cells accumulated lipid droplets, while, unexpectedly, PNPLA3^{KO} cells were highly steatotic with over 80% of cells accumulating lipid droplets.

Next, we measured the viability of the cells following PA treatment (Fig. 3A). As expected in PNPLA3^{UC} HLCs, OA treatment had minimal effect, whereas PA treatment resulted in profound loss of viability. On the other hand, PNPLA3^{KO} HLCs were far less sensitive to the PA-induced lipotoxicity and maintained high viability close to 80% when compared with untreated cells. The PNPLA3^{I148M} variant showed an intermediate phenotype. Additionally, we assessed the expression of endoplasmic reticulum (ER) stress markers. After 48 hours

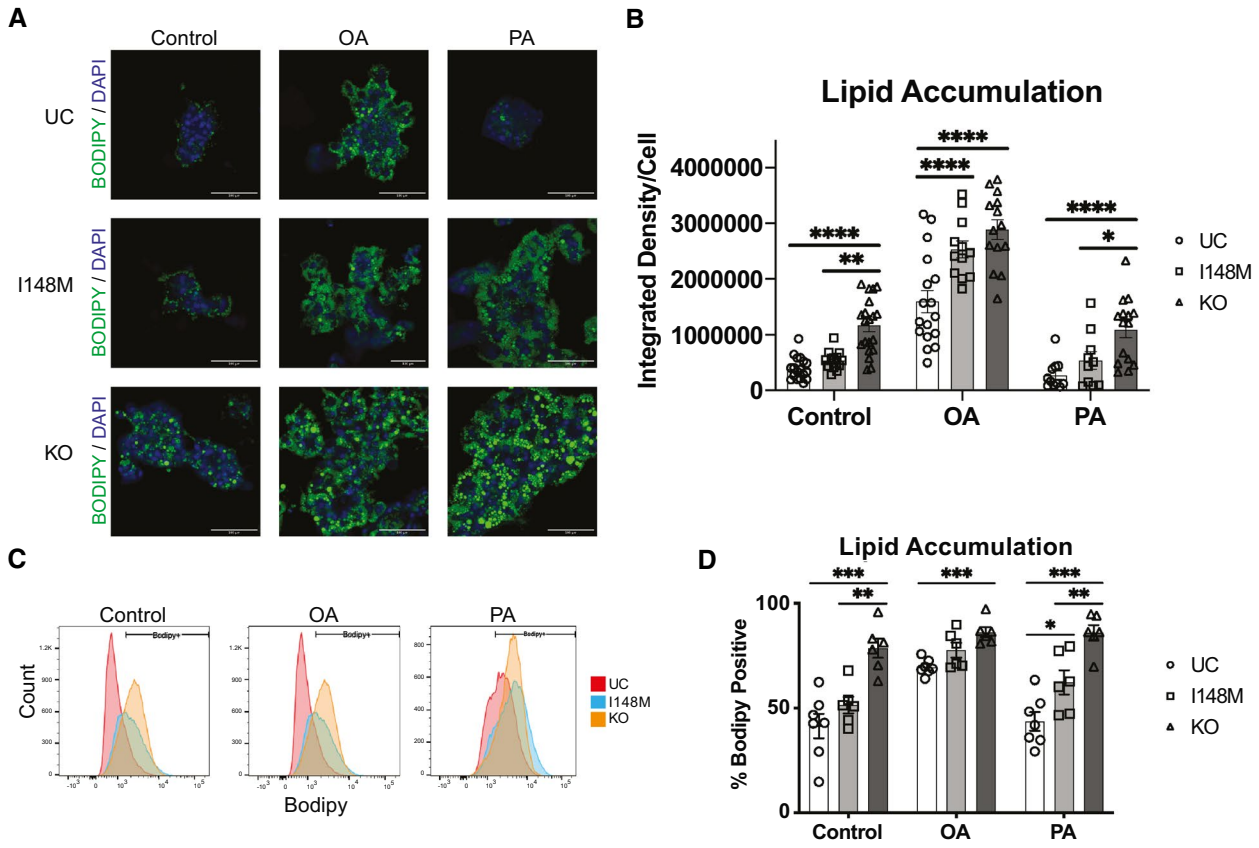

FIG. 2. PNPLA3-edited HLCs accumulate more lipid droplets than PNPLA3^{UC} HLCs. Cells were differentiated into HLCs, placed in 3D, and treated for 1 week with control, OA, or PA medium. Flow cytometric analyses were done using 2D cells. (A) Representative images of BODIPY-stained lipid droplets in cells from the three genotypes. Regardless of treatment type, progressively more lipids were accumulated in PNPLA3^{I148M} cells and PNPLA3^{KO} cells than PNPLA3^{UC} cells. (B) Quantification of the BODIPY staining intensity relative to cell number in (A) (PNPLA3^{UC}, n = 6 images per clone, 2 clones, and 2 independent experiments; PNPLA3^{I148M}, n = 6 images per clone, 2 clones, and 2 independent experiments; PNPLA3^{KO}, n = 6 images per clone, 2 clones, and 2 independent experiments). A two-way ANOVA with Tukey's multiple comparisons tests was performed to test statistical significance between means. Data are represented as mean ± SEM. (C) Representative flow cytometric analysis of lipid accumulation through BODIPY staining. (D) Quantification of the percentage of BODIPY-positive cells in (C) (PNPLA3^{UC}, n = 2 clones and 5 independent experiments; PNPLA3^{I148M}, n = 2 clones and 5 independent experiments; and PNPLA3^{KO}, n = 3 clones and 2 independent experiments). A two-way ANOVA with Tukey's multiple comparisons tests was performed to test statistical significance between means. Data are represented as mean ± SEM. There was a stepwise increase in lipid accumulation from PNPLA3^{UC} to PNPLA3^{I148M} to PNPLA3^{KO} cells. This increase in steatosis in the PNPLA3-edited cells is consistent with the disease phenotype. See also Supporting Figs. S5-S7.

of PA treatment, PNPLA3^{UC} cells up-regulated the cell stress markers binding immunoglobulin protein (BIP), growth arrest and DNA damage inducible protein (GADD34), C/EBP homologous protein (CHOP), and protein kinase R-like endoplasmic reticulum kinase (PERK) (Fig. 3B). The expression of these markers was significantly lower in PNPLA3^{KO} cells. Finally, we analyzed the mRNA expression and activation of CASP1 following 1 week of treatment (Fig. 3C,D). PNPLA3-edited HLCs failed to up-regulate CASP1 expression and activation in response to PA, indicating that these cells have an altered reaction to lipid-induced stress. We confirmed the major phenotypic findings in the second genetic background (Supporting Fig. S5). To confirm that PNPLA3-edited cells are resistant to saturated fatty acid (SFA)–induced stress, we performed similar experiments using SA. SA was slightly more steatogenic and slightly less lipotoxic, but generally we observed similar lipid accumulation, viability, and ER stress phenotypes as PA treatment (Supporting Fig. S6).

We also treated HLCs for 24 and 48 hours to determine how quickly the differences in lipid accumulation develop (Supporting Fig. S7). We found that the lipid accumulation phenotypes of the three genotypes were apparent even at the earliest timepoint. However, 1 week of PA treatment was necessary to produce lipotoxicity in PNPLA3^{UC} cells. This finding was not entirely unexpected, as NAFLD in a

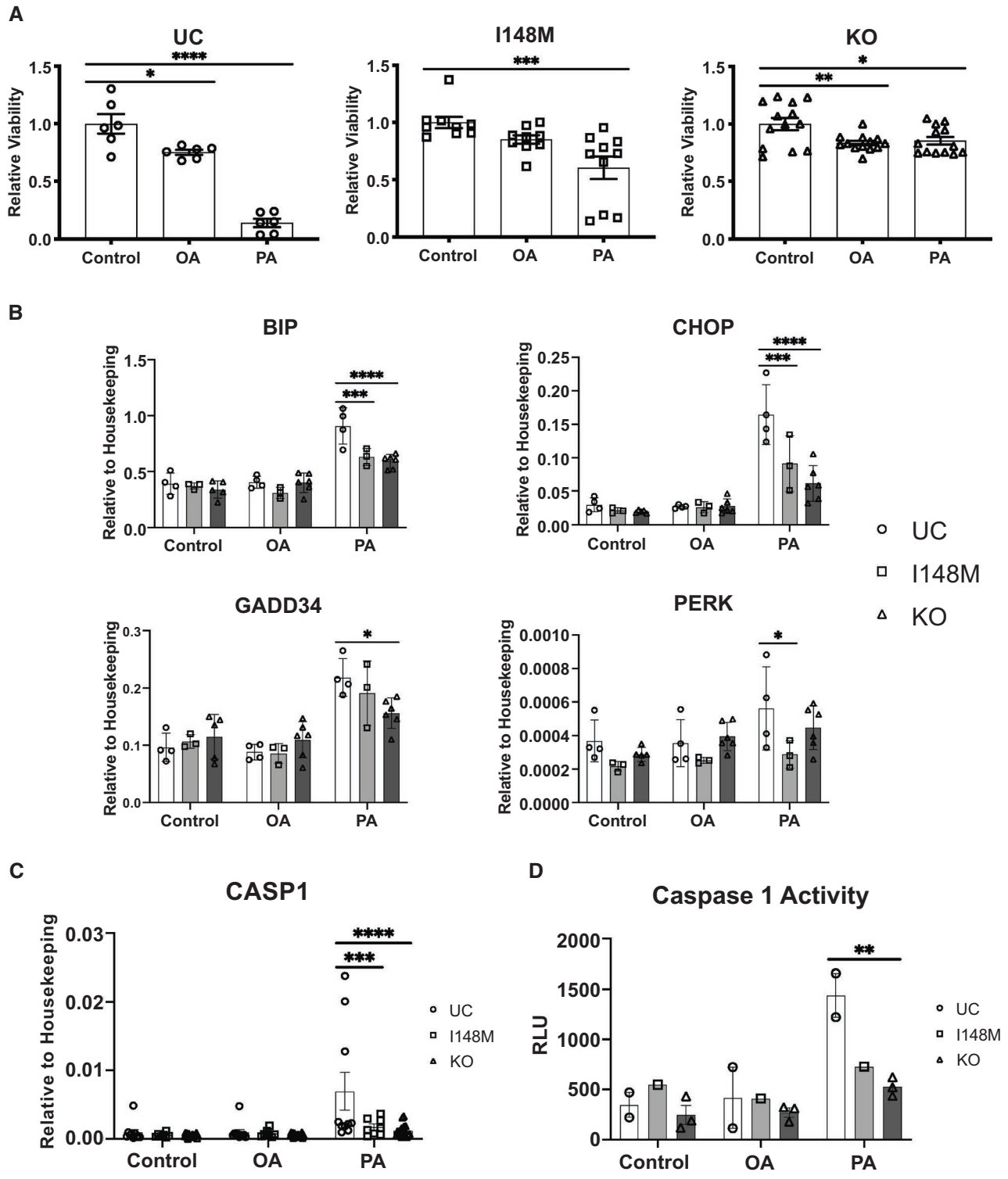

FIG. 3. PNPLA3-edited cells are resistant to PA-induced lipotoxicity. Cells were differentiated into HLCs, placed in 3D, and treated for 48 hours to 1 week with control, OA, or PA medium to assess the effect of fatty acid treatment on the viability of HLCs. (A) Relative viability of FFA-treated cells to control cells within each genotype ($PNPLA3^{UC}$, n = 2 clones and 3 independent experiments; $PNPLA3^{I148M}$, n = 2 clones and 7 independent experiments; and $PNPLA3^{KO}$, n = 3 clones and 5 independent experiments). Ordinary one-way ANOVA with Dunnett's multiple comparisons tests were performed to test statistical significance between means. Data are represented as mean ± SEM. $PNPLA3^{UC}$ cells are susceptible to PA lipotoxicity, while $PNPLA3^{KO}$ cells are resistant to this lipotoxic insult. $PNPLA3^{I148M}$ cells show an intermediate phenotype between them. (B) mRNA expression of ER stress markers BIP, GADD34, CHOP, and PERK following 48 hours of FFA treatment ($PNPLA3^{UC}$, n = 2 clones and 2 independent experiments; $PNPLA3^{I148M}$, n = 2 clones and 2 independent experiments; and $PNPLA3^{KO}$, n = 3 clones and 2 independent experiments). Two-way ANOVAs with Tukey's multiple comparisons tests were performed to test statistical significance between means. Data are represented as mean ± SEM. In $PNPLA3^{UC}$ cells, ER stress markers are induced by PA treatment. $PNPLA3^{I148M}$ and $PNPA3^{KO}$ cells are resistant the induction of ER stress markers following PA treatment. (C) mRNA expression of CASP1 following 1 week of FFA treatment ($PNPLA3^{UC}$, n = 2 clones and 6 independent experiments; $PNPLA3^{I148M}$, n = 2 clones and 6 independent experiments; and $PNPLA3^{KO}$, n = 3 clones and 6 independent experiments). Two-way ANOVAs with Tukey's multiple comparisons tests were performed to test statistical significance between means. Data are represented as mean ± SEM. (D) Caspase 1 activity in HLCs treated with FFAs for 1 week ($PNPLA3^{UC}$, n = 2 clones and 1 independent experiment; $PNPLA3^{I148M}$, n = 2 clones and 1 independent experiment; and $PNPLA3^{KO}$, n = 2 clones and 1 independent experiment). Two-way ANOVAs with Tukey's multiple comparisons tests were performed to test statistical significance between means. Data are represented as mean ± SEM. Treatment with PA induces the expression of CASP1 in $PNPLA3^{UC}$ cells, indicating that the PA-induced lipotoxicity is mediated through inflammasome activation and pyroptosis. PNPLA3-edited cells fail to up-regulate CASP1 expression in response to PA treatment. See also Supporting Figs. S5 and S6. Abbreviations: GADD34, growth arrest and DNA damage inducible protein; PERK, protein kinase R-like endoplasmic reticulum kinase.

chronic disease that takes years or decades to develop. Therefore, it is possible that prolonged exposure to maladaptive lipids is necessary to cause sufficient cellular stress to induce toxicity.

To determine the underlying mechanism driving the increased lipid accumulation in PNPLA3-edited cells, we chose to examine the expression of markers of the three major lipid-processing pathways: *de novo* lipogenesis (DNL), VLDL secretion, and β-oxidation (Supporting Fig. S8). We found no major differences between genotypes in the expression of DNL or VLDL secretion genes. However, PNPLA3-edited cells expressed significantly lower levels of several β-oxidation genes. This indicates that despite the higher abundance of lipids in PNPLA3-edited HLCs, these cells failed to up-regulate lipid metabolism pathways to catabolize and eliminate excess lipids.

PNPLA3 LOSS OF FUNCTION RESULTS IN AN INCREASED PRODUCTION OF TGS

Recent literature demonstrates an increasing appreciation for lipids as more than just metabolic byproducts.[24] Indeed, lipids often serve as signaling molecules, and lipidomic signatures can be used to differentiate between healthy and diseased individuals. Accordingly, carriers of the PNPLA3 I148M variant have a unique lipidomic signature that differentiates them from both healthy individuals and those with obesity-induced NAFLD.[25,26] To assess the effect of PNPLA3 genotype on lipid metabolism in our system, we performed lipidomic profiling. These analyses confirmed that FFA treatment alters the lipid signature, and more importantly that the PNPLA3 genotype had a major effect on HLCs' lipidomic profile. Principle component analysis (PCA) plots comparing $PNPLA3^{KO}$ and $PNPLA3^{UC}$ groups showed a complete separation among the genotypes regardless of treatment (Fig. 4A,C-E). An intermediate phenotype between the $PNPLA3^{UC}$ and $PNPLA3^{KO}$ HLCs was observed with $PNPLA3^{I148M}$ cells (Supporting Fig. S10). Heatmaps of the top 25 differentially abundant lipid species indicated that TGs were the species most responsible for these differences (Fig. 3B-E).

Lipidomic profiles revealed that $PNPLA3^{KO}$ HLCs had generally higher levels of TGs (Fig. 3F). Of note, PNPLA3-edited HLCs preferentially accumulated TGs containing four to nine double bonds regardless of lipid treatment. These data are consistent with previous findings that the I148M variant causes a reduction in lipid droplet remodeling capacity and results in hepatic retention of polyunsaturated fatty acids (PUFAs).[26] This pattern of PUFA accumulation in hepatic TG may have profound effects on lipid metabolism: PUFAs inhibit sterol regulatory element binding protein 1c, causing the down-regulation of DNL, which is characteristic of patients with the I148M variant. This reduction in DNL may prevent the accumulation of toxic intermediates that contribute to lipotoxicity and insulin

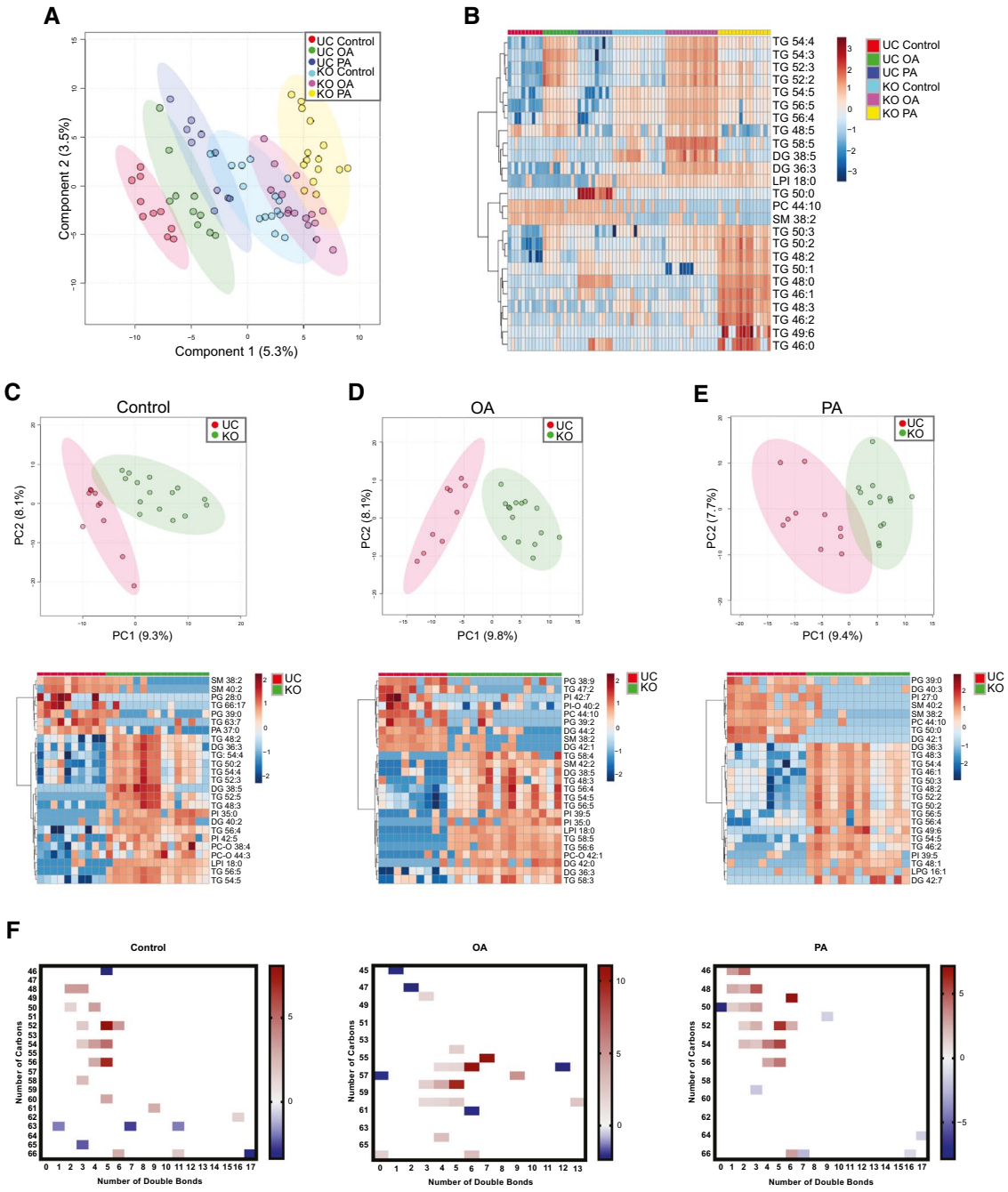

FIG. 4. Lipidomic comparison of PNPLA3^{UC} and PNPLA3^{KO} following FFA treatment. Lipidomic differences between PNPLA3^{UC} and PNPLA3^{KO} cells treated with control, OA, and PA media for 1 week were analyzed (PNPLA3^{UC}, n = 2 clones [with 5 technical replicates] and 1 independent experiment; PNPLA3^{KO}, n = 3 clones [with 5 technical replicates] and 1 independent experiment). (A) Projection to latent structure discriminant analysis plot of the six experimental groups. The two genotypes cluster separately, with slight differences attributable to the FFA treatment within each genotype. (B) Heatmap of the top 25 differentially abundant lipid species in all six experimental groups. The lipid species most responsible for lipidomic differences between groups is TGs. PCA plot and heatmap of the top 25 differentially abundant lipid species comparing the effect of control medium (C), OA medium (D), and PA medium (E) on genotypic differences. Regardless of treatment, PNPLA3^{UC} and PNPLA3^{KO} cells clustered far apart from one another. Once again, TGs were a major determinant in driving lipidomic differences among the groups. (F) Heatmaps showing the $\log_2$-fold change difference in abundance of TGs that were statistically differentially abundant between PNPLA3^{UC} and PNPLA3^{KO} cells following the three treatments. In the PA treatment group, this analysis indicates that PNPLA3^{KO} cells may be preferentially incorporating SFAs into TGs, as a plurality of TGs that are differentially abundant between the two groups possess less than three double bonds. See also Supporting Figs. S9 and S10.

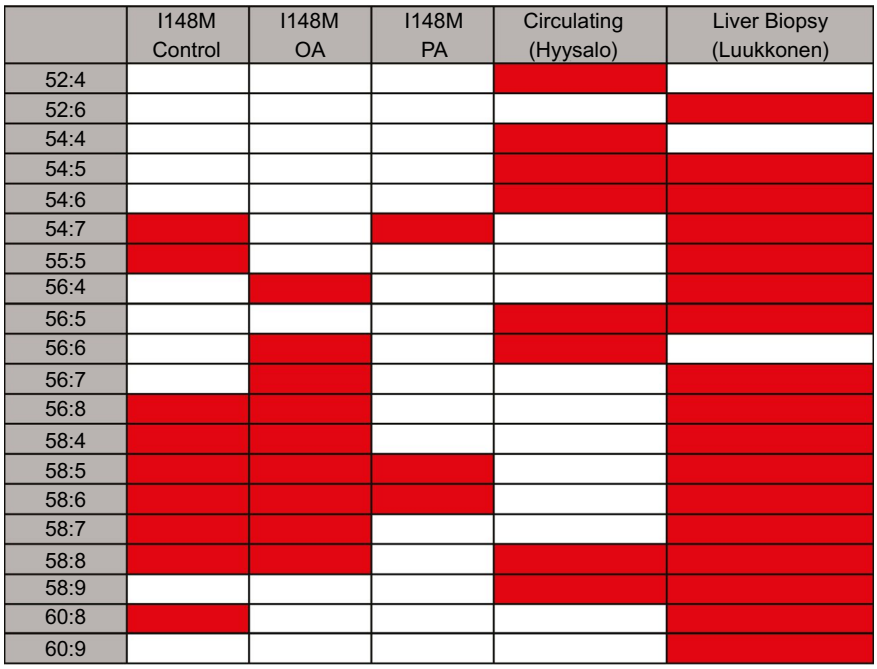

FIG. 5. PNPLA3^{I148M} cells mirror lipidomic profile of liver biopsies from homozygous PNPLA3 I148M carriers. Table shows up-regulated TG species of PNPLA3 I148M carriers in circulating samples (Hyysalo et al.) and liver biopsies (Luukkonen et al.) compared with PNPLA3^{I148M} lipidomic samples. The PNPLA3^{I148M} lipidomic profile more closely resembles the profile of liver biopsies from patients with PNPLA3 I148M than the circulating lipidomic profile. The significant overlap (12 of 17 species) between our system and patient samples indicates the biological relevance of this system for modeling PNPLA3-induced NAFLD.

resistance. Therefore, the preferential accumulation of PUFA-containing TG species may be cytoprotective against the ER stress caused by lipid overload in these cells. Additionally, the TG profile of PA-treated cells revealed that PNPLA3^{KO} HLCs incorporated more SFAs into TGs than PNPLA3^{UC} HLCs (Fig. 4F and Supporting Fig. S10F). In support of the hypothesis that PNPLA3 is a major lipid droplet remodeling protein, we found that PNPLA3-edited HLCs significantly down-regulate the expression of several lipid droplet markers (Supporting Fig. S8). Thus, loss of PNPLA3 functionality could result in dysregulated lipid droplet remodeling, which causes alterations to the lipid pool as well as the protein coating of lipid droplets.

To contextualize our model in terms of the human disease, we compared the lipidomic profile of PNPLA3^{I148M} cells with published data of both the circulating[25] and hepatic lipidomic profiles[26] of homozygous PNPLA3 I148M carriers (Fig. 5). Given that TGs were the lipid species with the largest difference in the lipidomic profile of our cells, we confined our analysis to TGs. We found that of the 20 TG species that were up-regulated in I148M carriers, 12 were similarly up-regulated in the PNPLA3^{I148M} cells. This analysis indicated that PNPLA3^{I148M} cells closely resemble the lipidomic profile of liver biopsies from I148M carriers. Of the 12 TGs that were up-regulated in PNPLA3^{I148M} HLCs, 10 were exclusively found in the lipidomic samples from patient liver biopsies. The TG species that were common between our system and the patients were all PUFAs. This result offers clinical validation of our system, as we were able to recapitulate major aspects of the PNPLA3-induced NAFLD phenotype in humans. To conclude, loss of function of PNPLA3 results in major modification in lipidomic profile of HLCs, suggesting an improved transformation of FFAs into TGs as well as reduced lipid droplet remodeling capacity.

TRANSCRIPTOMIC ANALYSES REVEAL THAT LOSS OF FUNCTION IN PNPLA3 BROADLY AFFECTS LIPID METABOLISM IN HLCS

To further uncover the molecular mechanisms involved in the PNPLA3 phenotype, we performed RNA-sequencing (RNA-Seq) analyses on HLCs grown in the presence of FFAs. The resulting data

sets were analyzed using PCA and showed that regardless of treatment, PNPLA3^{UC} HLCs displayed a different transcriptomic profile when compared with PNPLA3^{KO} cells, while PNPLA3^{I148M} cells appeared to have an intermediate profile (Fig. 6A). This observation was further confirmed by heatmap analyses of the top 500 differentially expressed genes between PNPLA3^{KO} and PNPLA3^{UC} HLCs in each treatment (Fig. 6B and Supporting Table S5). These data indicated that the PNPLA3 genotype

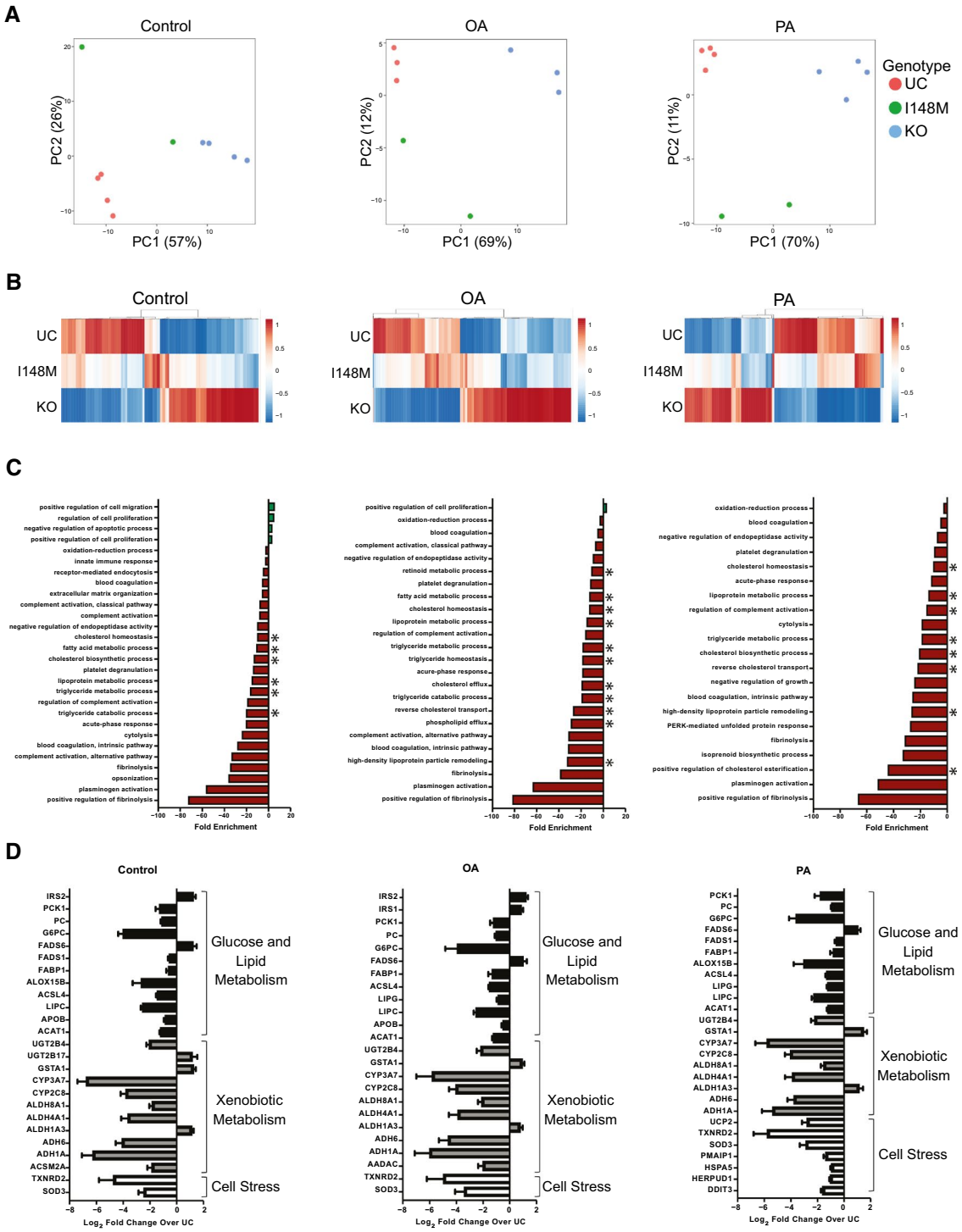

FIG. 6. The intermediate phenotype of PNPLA3^{I148M} indicates that the variant may be loss of function. Transcriptomic differences among PNPLA3^{UC}, PNPLA3^{I148M}, and PNPLA3^{KO} cells treated with control, OA, and PA media for 24 hours were analyzed (PNPLA3^{UC}, n = 2 clones and 2 independent experiments; PNPLA3^{I148M}, n = 1 clones and 2 independent experiments; and PNPLA3^{KO}, n = 2 clones and 2 independent experiments). (A) PCA plots comparing the three genotypes following the respective treatments. Regardless of treatment, PNPLA3^{UC} and PNPLA3^{KO} cells clustered far apart from one another, whereas PNPLA3^{I148M} cells are positioned between the two, indicating that it represents an intermediate phenotype. (B) Heatmaps of the top 500 differentially expressed genes between PNPLA3^{UC} and PNPLA3^{KO} cells for each treatment. This once again shows that PNPLA3^{I148M} cells have a transcriptomic expression profile that is intermediate between those of PNPLA3^{UC} cells and PNPLA3^{KO} cells. (C) Gene ontology enrichment analysis comparing PNPLA3^{UC} and PNPLA3^{KO} cells. Statistically significantly up-regulated pathways are shown in green, and down-regulated pathways are shown in red. Metabolic processes are highlighted with a star. These results indicate that PNPLA3^{KO} cells down-regulate several metabolic pathways compared with PNPLA3^{UC} cells, regardless of treatment type. (D) Log_2-fold change expression of selected differentially expressed genes in PNPLA3^{KO} cells compared with PNPLA3^{UC} cells. Lipid and glucose metabolism genes are shown in black; xenobiotic metabolism genes are shown in gray; and cell stress genes are shown in white. Generally, PNPLA3^{KO} cells down-regulate genes involved in each of the these pathways compared with PNPLA3^{UC} cells, regardless of treatment type. See also Supporting Fig. S11.

fundamentally alters the transcriptomic profile of HLCs, while lipid treatment merely exacerbates the underlying phenotype. This finding is consistent with our findings showing that PNPLA3-edited cells demonstrated increased lipid accumulation and altered lipidomic profiles at baseline.

The top 500 differentially expressed genes between PNPLA3^{UC} and PNPLA3^{KO} in each treatment group were then subjected to Gene Ontology pathway analysis (Fig. 6C), which highlighted a profound down-regulation of several metabolic pathways in the PNPLA3^{KO} cells. After closer inspection, we found that in addition to lipid metabolism, PNPLA3^{KO} HLCs down-regulated genes responsible for glucose metabolism, xenobiotic metabolism, and cell stress (Fig. 6D). Interestingly, insulin receptor signaling appeared to be up-regulated, which could explain a decrease in genes involved in glycogenolysis and gluconeogenesis (*PCK1*, *PC*, and *G6PC*). This finding indicated that PNPLA3^{KO} cells may maintain insulin sensitivity in spite of steatosis, which is consistent with the clinical characteristics of I148M carriers. Additionally, the expression of several lipid droplet–remodeling proteins was altered in PNPLA3^{KO} cells. The fatty acid desaturase 6 (*FADS6*) gene, which is responsible for desaturating fatty acids, was up-regulated, while the lipolytic enzymes LIPC and LIPG were down-regulated. This expression pattern supports the hypothesis that PNPLA3 is a lipid droplet–remodeling protein, and loss of this function fundamentally alters lipid droplet dynamics.

In addition to lipid and glucose metabolism, PNPLA3^{KO} HLCs also down-regulated genes responsible for all three phases of drug metabolism. These genes included, but were not limited to, the CYP, UGT, and SLC families of enzymes. In accordance with our finding that PNPLA3^{KO} cells are resistant to PA-induced lipotoxicity, we found that these cells tended to exhibit lower expression of several key cell stress markers including UCP2, SOD3, BIP, and CHOP.

PCA of the RNA-Seq data among the genotypes in response to FFA (Supporting Fig. S11) showed that PA treatment had the strongest effect on the gene-expression profile of PNPLA3^{UC} HLCs. Interestingly, both PNPLA3^{I148M} and PNPLA3^{KO} HLCs did not cluster separately based on treatment type. Taken together, these data show that absence of PNPLA3 or the presence of the I148M variant profoundly changes the gene expression of HLCs, which in turn alters their capacity to react against lipid stressors. Thus, the transcriptomic similarities between PNPLA3 genotypes reinforce our observation that the I148M variant represents a loss of function.

Of note, the transcriptomic profile of our PNPLA3-edited HLCs also mimicked that of patients carrying the I148M variant. In a study analyzing the transcriptomic differences between carriers and noncarriers of the I148M variant, Baselli et al. found that carriers down-regulated oxidative phosphorylation, fatty acid metabolism, and xenobiotic metabolism.[27] These data offer further clinical validation of our hypotheses that the I148M variant disrupts cellular metabolism on a global scale, leading to reduced lipid and xenobiotic metabolism.

BLOCKING TG FORMATION RESENSITIZES PNPLA3^{KO} CELLS TO PA-INDUCED TOXICITY

Based on these results, we hypothesized that the reduced β-oxidation and increased incorporation of

harmful SFAs into TGs could represent the mechanism by which PNPLA3^{KO} HLCs reduce SFA-induced lipotoxicity. Accordingly, it has been shown previously that shuttling SFAs into TGs instead of other metabolic processes results in decreased lipotoxicity.[28] To test this hypothesis, we blocked TG synthesis in HLCs treated with PA using small molecule inhibitors. Because it is unknown where in the TG enzyme cascade PNPLA3 might act, two inhibitors were chosen: triacsin C to block GPAT at the top of the enzyme cascade, and T863 to block DGAT at the bottom of the cascade. Both triacsin C and T863 significantly reduced lipid droplet accumulation in HLCs treated with either OA (Supporting Fig. S12) or PA (Fig. 7A,B). Viability of HLCs treated with PA + DMSO, PA + triacsin C, and PA + T863 was then assessed (Fig. 7C). In PNPLA3^{UC} HLCs, the addition of the inhibitors had no effect on cell death induced by PA treatment. On the other hand, addition of triacsin C and T863 resulted in a statistically significant reduction in viability in PNPLA3^{KO} HLCs grown in the presence of PA. Once again, PNPLA3^{I148M} HLCs showed an intermediate phenotype between PNPLA3^{UC} and PNPLA3^{KO} cells. These findings were confirmed in a second genetic background (Supporting Fig. S11). Together, these results indicate that blocking TG formation could, in part, resensitize PNPLA3^{KO} cells to PA-induced toxicity. However, given that the increased toxicity by blocking TG formation was not observed in PNPLA3^{UC} cells when treated with PA, additional mechanisms may contribute to the resistance of PNPLA3^{KO} cells to lipid-induced stress.

LOSS OF PNPLA3 FUNCTION RESULTS IN INCREASED SUSCEPTIBILITY TO ETHANOL TOXICITY

To explore the mechanism of PNPLA3^{KO} and PNPLA3^{I148M} genotypes in liver injury in addition to steatosis, we hypothesized that the increased lipid loading in these cells along with their altered lipid and xenobiotic metabolism would make them more susceptible to other forms of toxicity. We chose to test this hypothesis using ethanol and methotrexate, whose hepatotoxic effects may be modulated by PNPLA3 genotype.[29,30] Descriptions of the treatment timeline can be found in Fig. 8A,C. PNPLA3^{KO} HLCs were significantly less viable than PNPLA3^{UC} cells after ethanol/TNF or methotrexate treatment, whereas PNPLA3^{I148M} cells displayed an intermediate sensitivity (Fig. 8B,D). Even though the concentrations of both hepatotoxins were relatively nontoxic to PNPLA3^{UC} cells, they induced a high level of cell death in PNPLA3^{KO} HLCs. The increased susceptibility of PNPLA3-edited cells to ethanol-induced hepatotoxicity was confirmed in the second genetic background (Supporting Fig. S13). The increased toxicity is likely driven by the lower expression of drug metabolizing enzymes that play a role in detoxification of these hepatotoxins (Fig. 8E). Ethanol toxicity has been shown to be dependent on the activation of stress kinases, including p-JNK and pp38-MAPK.[31,32] The expression of these two kinases was highly induced in PNPLA3^{KO} HLCs following ethanol and TNF treatment, while the PNPLA3^{UC} HLCs were relatively resistant to this induction, mirroring the genotypes' susceptibility to toxicity (Fig. 8F,G). Importantly, PNPLA3^{KO} HLCs expressed a higher basal level of both kinases, which may explain their increased susceptibility to hepatotoxicity. These findings suggest that changes in PNPLA3 activity increase susceptibility to hepatotoxic agents, thereby explaining the contribution of the I148M variant to the progression of the disease toward NASH.

Discussion

Using our hiPSCs model system, we demonstrated that changes in PNPLA3 activity have major effects on the metabolic activity of human hepatocytes, which may in turn influence the progression of NAFLD. This study report in a human hepatic system that the I148M variant in the PNPLA3 gene leads to NAFLD disease progression through a loss of function mutation. Our data indicate that loss of PNPLA3 activity leads to increased steatosis and resistance to SFA-induced cell stress *in vitro*. This latter phenotype is counter-intuitive, at least in part, due to the down-regulation of lipid metabolism that leads to excessive diversion of SFAs into TGs. More importantly, loss of PNPLA3 leads to the down-regulation of xenobiotic metabolism in hepatocytes, making them more susceptible to other hepatotoxins such as ethanol. Thus, subclinical but sustained damage to the livers of these patients caused by environmental hepatotoxins may result in disease progression to NASH.

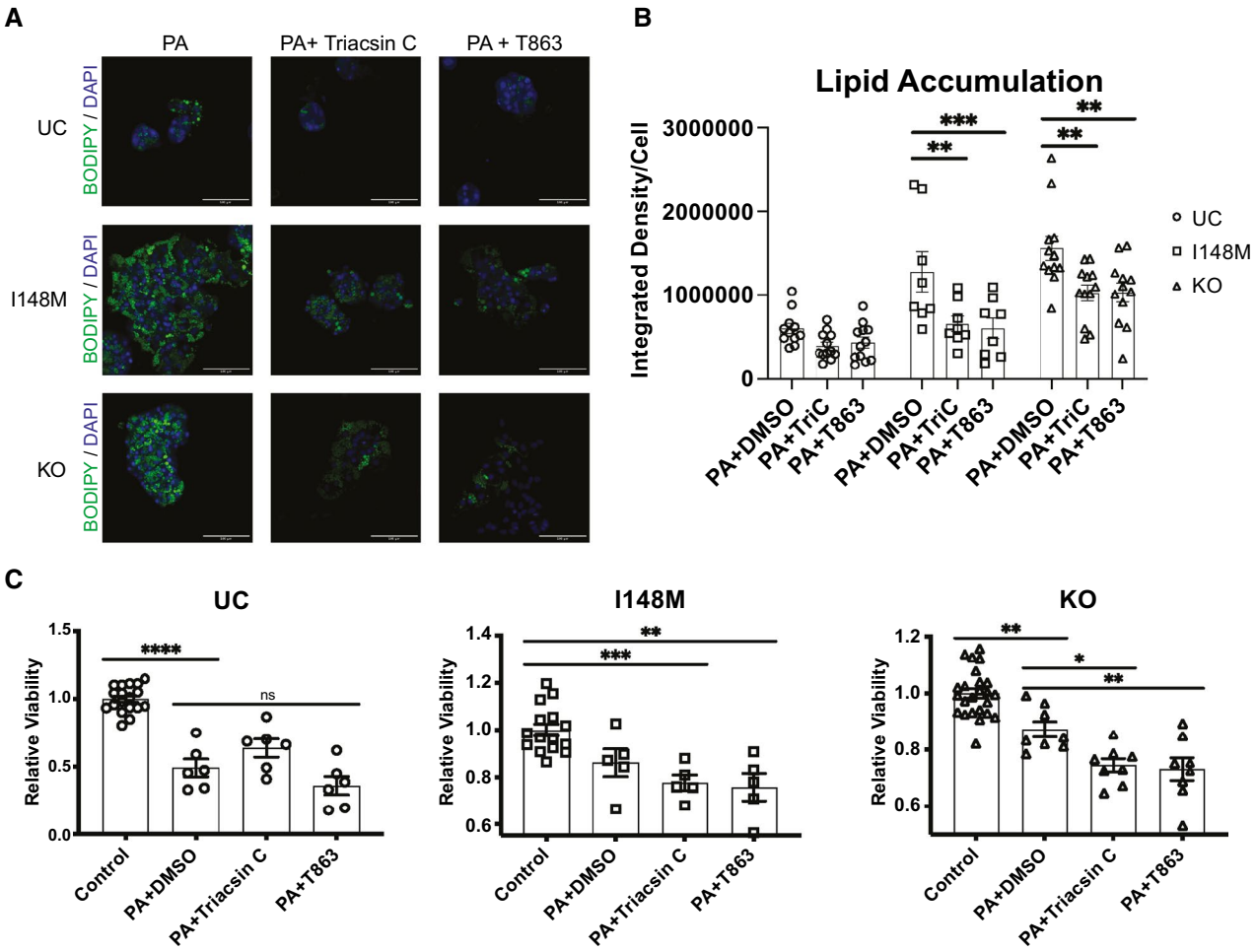

FIG. 7. Blocking TG formation resensitizes PNPLA3^{KO} cells to PA-induced lipotoxicity. TG formation was blocked using small molecule inhibitors triacsin C and T863. (A) Representative images of BODIPY lipid staining following 1 week of treatment with PA and PA supplemented with the respective inhibitors. (B) Quantification of the BODIPY staining intensity relative to cell number in (A) (PNPLA3^{UC}, n = 4 images per clone, 2 clones, and 3 independent experiments; PNPLA3^{I148M}, n = 4 images per clone, 2 clones, and 2 independent experiments; and PNPLA3^{KO}, n = 4 images per clone, 2 clones, and 2 independent experiments). A two-way ANOVA with Tukey's multiple comparisons tests was performed to test statistical significance between means. Data are represented as mean ± SEM. Lipid accumulation was incompletely inhibited by both inhibitors in all three genotypes. (C) Relative viability of PA and PA + inhibitor–treated cells to control treated cells within each genotype (PNPLA3^{UC}, n = 2 clones and 3 independent experiments; PNPLA3^{I148M}, n = 1 clone and 4 independent experiments; and PNPLA3^{KO}, n = 2 clones and 4 independent experiments). Ordinary one-way ANOVAs with Dunnett's multiple comparisons tests were performed to test the statistical significance between means. Data are represented as mean ± SEM. For PNPLA3^{UC} cells, treatment with PA resulted in a significant loss of viability, but treatment with the TG inhibitors did not result in additional loss of viability. However, treatment with both inhibitors resulted in a significant reduction in viability for PNPLA3^{KO} cells. PNPLA3^{I148M} cells showed an intermediate phenotype with a slight reduction in viability when treated with the TG inhibitors that did not reach significance. See also Supporting Fig. S12.

Importantly, previous genetic studies in the mouse have shown that absence of PNPLA3 does not result in a NAFLD-like phenotype.[12] However, when either the I148M PNPLA3 protein or a catalytically dead version of PNPLA3 (S47A) are overexpressed in mouse livers, these mutant proteins accumulate on the surfaces of lipid droplets, which may restrict either cofactors or lipid mobility. As a consequence, the effect of the I148M variant is often considered a gain of function. Accordingly, multiple companies are now developing PNPLA3 inhibitors to limit NAFLD aggravation based on these observations.[33] However, this finding fails to account for the substantial sequence divergence of mouse and human PNPLA3

genes as well as the differences in tissue localization of PNPLA3 between these species. Indeed, PNPLA3 is endogenously expressed at extremely low levels in mouse livers and high levels in adipose tissue.[9,13,14] Accordingly, it has been shown that PNPLA3 must be overexpressed in liver tissue for a phenotype to be observed.[34]

Importantly, previous *in vitro* studies as well as some studies in human cohorts have demonstrated that the I148M variant leads to a loss of enzymatic

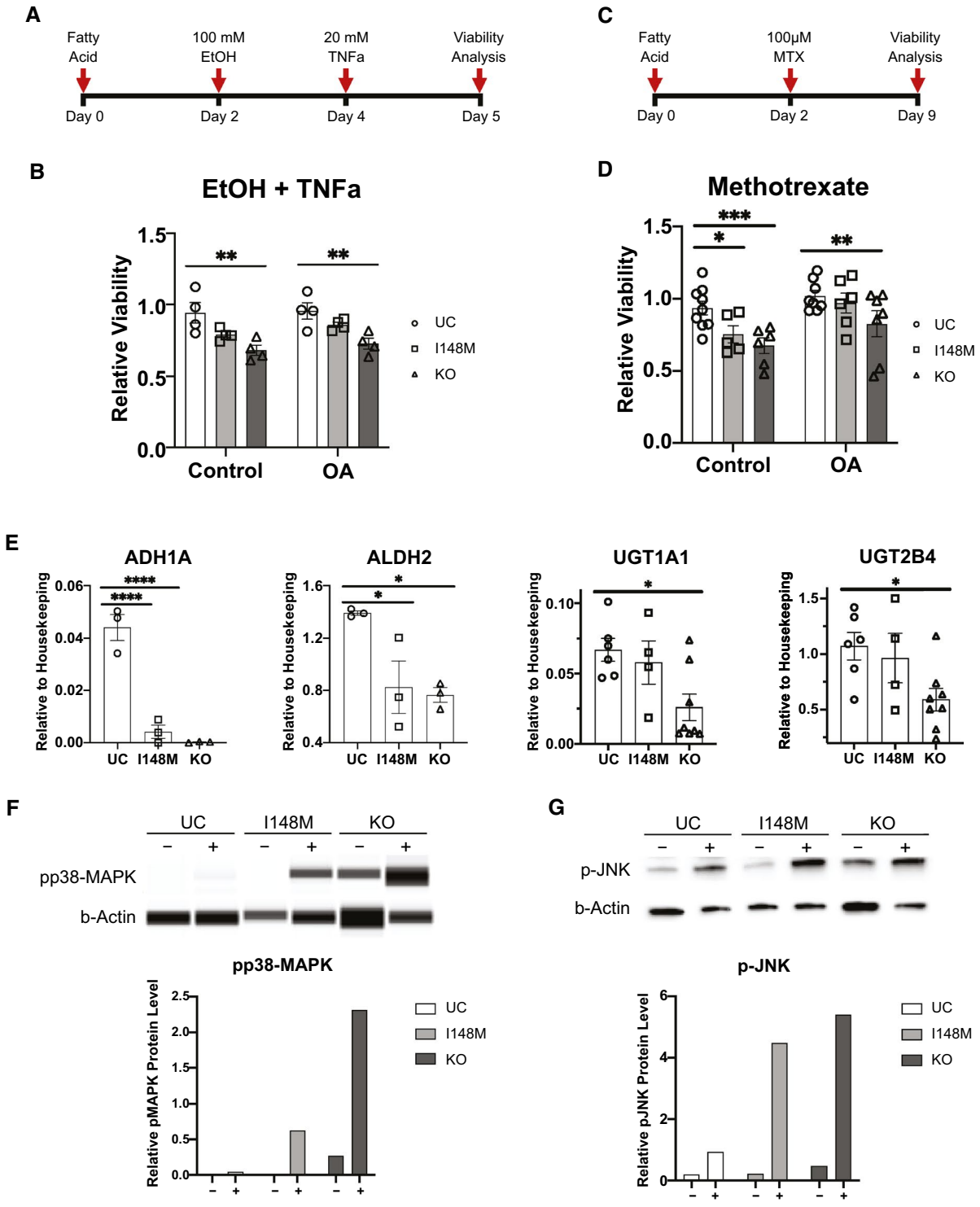

FIG. 8. Loss of PNPLA3 function results in increased susceptibility to ethanol and methotrexate toxicity. (A) Timeline of ethanol + TNFa treatment to induce toxicity. (B) Relative viability of ethanol + TNFa–treated cells to untreated cells within each genotype ($PNPLA3^{UC}$, n = 2 clones and 2 independent experiments; $PNPLA3^{I148M}$, n = 2 clones and 2 independent experiments; and $PNPLA3^{KO}$, n = 2 clones and 2 independent experiments). A two-way ANOVA with Tukey's multiple comparisons tests was performed to test statistical significance between means. Data are represented as mean ± SEM. Given the sublethal does of ethanol given, $PNPLA3^{UC}$ cells retained high viability following treatment. Conversely, $PNPLA3^{KO}$ cells showed an acute toxicity when treated with even a sublethal dose of ethanol. $PNPLA3^{I148M}$ cells were intermediate between $PNPLA3^{UC}$ and $PNPLA3^{KO}$ cells. This trend was consistent in both control and OA-treated cells, indicating that this effect may be independent of steatosis. (C) Timeline of methotrexate treatment to induce toxicity. (D) Relative viability of methotrexate treated cells to untreated cells within each genotype ($PNPLA3^{UC}$, n = 2 clones and 6 independent experiments; $PNPLA3^{I148M}$, n = 2 clones and 3 independent experiments; and $PNPLA3^{KO}$, n = 2 clones and 4 independent experiments). A two-way ANOVA with Tukey's multiple comparisons tests was performed to test statistical significance between means. Data are represented as mean ± SEM. (E) mRNA expression of the drug metabolizing enzymes ADH1A, ALDH2, UGT1A1, and UGT2B4 among the three genotypes ($PNPLA3^{UC}$, n = 2 clones and 2 independent experiments; $PNPLA3^{I148M}$, n = 2 clones and 2 independent experiments; and $PNPLA3^{KO}$, n = 2 clones and 2 independent experiments). Ordinary one-way ANOVAs with Dunnett's multiple comparisons tests were performed to test statistical significance between means. Data are represented as mean ± SEM. PNPLA3-edited cells express significantly lower levels of these drug-metabolizing enzymes that are relevant for ethanol and methotrexate metabolism. The lower expression of these drug metabolizing enzymes may contribute to the increased toxicity burden in these genotypes. (F) Representative western blot and quantification graph showing protein expression of pp38-MAPK in the three genotypes with (+) and without (-) treatment with ethanol and TNF ($PNPLA3^{UC}$, n = 1 clone and 2 independent experiments; $PNPLA3^{I148M}$, n = 2 clones and 2 independent experiments; and $PNPLA3^{KO}$, n = 2 clones and 2 independent experiments). This experiment was performed using the protein simple whole-exome sequencing machine. (G) representative western blot and quantification graph showing protein expression of p-JNK in the three genotypes with (+) and without (-) treatment with ethanol and TNF ($PNPLA3^{UC}$, n = 1 clone and 2 independent experiments; $PNPLA3^{I148M}$, n = 2 clones and 2 independent experiments; and $PNPLA3^{KO}$, n = 2 clones and 2 independent experiments). This experiment was performed using standard western blotting techniques. See also Supporting Fig. S13.

activity.[26,35] Of particular interest, Luukkonen et al. showed that knocking out PNPLA3 results in lipid accumulation in the immortalized skin cell line A431.[26] Additionally, Romeo et al. found that patients with mutations in the PNPLA3 gene that were likely to be null presented with a phenotype closely resembling the I148M carriers.

It should be noted that one study did identify that the rs2294918 SNP in PNPLA3, which is associated with lower expression of PNPLA3, caused a slight improvement in NAFLD-associated traits in carriers of the I148M variant. However, this study also found that in reducing the expression of the wild-type PNPLA3 enzyme, the rs2294918 SNP reduced the protective effect of the wild-type allele against NAFLD development and progression. This finding implies that reduced expression of PNPLA3 protein predisposes patients to NAFLD and offers further evidence that reduced PNPLA3 expression and/or functionality is pathogenic. Although there are profound interspecies differences in the functionality and pathogenicity of PNPLA3 between mice and humans, some data from murine models do support the hypothesis that I148M is a loss of function variant. Indeed, overexpression of a catalytically dead version of PNPLA3 results in a similar phenotype as overexpression of the I148M variant,[26,35] indicating that the I148M variant is equivalent to loss of PNPLA3 catalytic function in mouse livers. Taken together, these findings support our conclusion that the I148M variant is a loss-of-function mutation that leads to more severe NAFLD in human.

The I148M variant in PNPLA3 has been shown in more than 50 studies to be robustly correlated with the full spectrum of NAFLD from simple steatosis through NASH, fibrosis, cirrhosis, and HCC.[6] However, the molecular mechanism by which this variant contributes to NAFLD remains unclear. As expected, the I148M variant caused an increase in lipid accumulation in our system. This finding is in direct agreement with the clinical evidence. However, our data also show that the variant is protective against saturated SFA-induced cell stress *in vitro*. Because the variant has been linked to worsening disease progression, this finding seems contradictory. There are several reasonable explanations for this apparent discrepancy.

First, SFAs exert their maladaptive effects *in vivo* by exacerbating insulin resistance. Selective insulin resistance leading to oxidative stress, mitochondrial dysfunction, and inflammation is a hallmark of NAFLD caused by metabolic disease.[36-38] Conversely, carriers of the I148M variant have lower levels of DNL and maintain insulin sensitivity despite high-grade

steatosis and liver injury.[4,25,39,40] Therefore, the resistance of PNPLA3-edited HLCs to SFA-induced cell stress may be more indicative of the intact insulin signaling pathway rather than true resistance to lipotoxic injury—a distinction that is difficult to discern in an *in vitro* system.[23,37] Furthermore, the pathogenesis of NASH is likely multifactorial and not simply explained by a direct lipotoxic effect of SFAs. Clinical studies indicate that the NAFLD disease profile of I148M carriers is different from that of NAFLD caused by obesity and metabolic syndrome. Consequently, it is reasonable to hypothesize that lipid-induced injury may occur via a mechanism other than saturated SFA-induced lipotoxicity and insulin resistance in carriers of the I148M variant compared to NAFLD patients with metabolic syndrome.

Second, our functional studies show that concomitant down-regulation of lipid and xenobiotic metabolism pathways causes the PNPLA3-edited cells to be more susceptible to other forms of toxicity. This model is consistent with the widely accepted concept that environmental factors modulate the effect of genetic variants on disease progression of NAFLD. Indeed, the I148M variant has been clinically linked to several detoxification diseases, including alcohol-associated liver disease, hereditary hemochromatosis, and drug-induced liver damage.[29,30,41] Thus, we propose that the I148M variant in PNPLA3 accelerates the progression toward NASH by increasing sensitivity of hepatocytes to common hepatotoxic compounds such as alcohol.

Finally, NAFLD is a complex metabolic disease that involves intercellular signaling among several hepatic cell types as well as extrahepatic tissues. PNPLA3 is known to be expressed in several cell types that are relevant to NAFLD, including hepatocytes, stellate cells, and macrophages.[42] Thus, we cannot exclude that PNPLA3 may affect complex cell–cell interactions involved in fibrosis and cirrhosis. Interestingly, our system offers the opportunity to dissect the role of PNPLA3 pathogenesis on hepatocytes from the other hepatic cells. Given the complex nature of this disease, it is possible that PNPLA3 differentially affects several hepatic cell types to manifest different aspects of the disease. *In vitro* studies indicate that PNPLA3 plays a role in the activation of hepatic stellate cells, and the I148M variant causes increased expression of proinflammatory and profibrotic markers as well as higher proliferation rate and chemotaxis.[10,42-44] Additionally, the I148M variant in PNPLA3 confers increased risk for fibrosis independent of other markers of disease severity.[45,46] Therefore, it is possible that the increased liver injury in I148M carriers is due to the proinflammatory and profibrotic phenotype of HSCs, whereas the increased steatosis in the hepatocytes of these patients is a distinct phenomenon. Further studies involving coculture of the different cell types mentioned previously could address this question. Given the unique properties of hiPSCs, the cell lines developed in this study could be used to develop such a complex culture system.

In summary, our study offers insight into the functionality of PNPLA3 and its pathophysiology in NAFLD. We believe that this *in vitro* system represents a platform to elucidate the full pathophysiology of the PNPLA3 I148M variant in NAFLD as well as drug development, while minimizing the reliance on live animal models. Our findings may have major implications for patient management. Indeed, decreasing PNPLA3 activity by pharmacological means may be a problematic therapeutic approach, as it could increase the risk of liver injury, and patients carrying the I148M could benefit from lifestyle modifications excluding alcohol or other hepatotoxins.

Acknowledgment: The authors thank the National Institute of Diabetes and Digestive and Kidney Diseases (NIDDK) Genomics Core, especially Harold Smith and Ilhan Akan, for assistance with the RNA-sequencing experiments. The authors also acknowledge Jeff Reece of the NIDDK Advanced Light Microscopy and Image Analysis Core for assistance with the confocal microscopy, and Bin Gao of the National Institute on Alcohol Abuse and Alcoholism for advice on ethanol-induced cytotoxicity.

Author Contributions: S.G.T contributed to the study concept, methodology, investigation, analysis, manuscript draft, review, and editing. C.M.M. contributed to the study concept, methodology, investigation, and manuscript review and editing. L.V. contributed to the study concept, methodology, investigation, manuscript review and editing, study supervision, and funding acquisition. T.J.L contributed to the study concept, manuscript review and editing, study supervision, and funding acquisition. A.S.L. contributed to the methodology and investigation. S.B.P. contributed to the investigation. Z.H., B.J., and A.K. contributed to the study resources.

REFERENCES

1) Bellentani S. The epidemiology of non-alcoholic fatty liver disease. Liver Int 2017;37(Suppl 1):81-84.
2) Younossi ZM, Stepanova M, Afendy M, Fang Y, Younossi Y, Mir H, Srishord M. Changes in the prevalence of the most common causes of chronic liver diseases in the United States from 1988 to 2008. Clin Gastroenterol Hepatol 2011;9:524-530.e1; quiz e60.
3) Anstee QM, Day CP. The genetics of NAFLD. Nat Rev Gastroenterol Hepatol 2013;10:645-655.
4) Kantartzis K, Peter A, Machicao F, Machann J, Wagner S, Konigsrainer I, et al. Dissociation between fatty liver and insulin resistance in humans carrying a variant of the patatin-like phospholipase 3 gene. Diabetes 2009;58:2616-2623.
5) Speliotes EK, Butler JL, Palmer CD, Voight BF, GIANT Consortium the MIGen Consortium, NASH CRN, Hirschhorn JN. PNPLA3 variants specifically confer increased risk for histologic nonalcoholic fatty liver disease but not metabolic disease. Hepatology 2010;52:904-912.
6) Dongiovanni P, Donati B, Fares R, Lombardi R, Mancina RM, Romeo S, et al. PNPLA3 I148M polymorphism and progressive liver disease. World J Gastroenterol 2013;19:6969-6978.
7) **Romeo S**, **Kozlitina J**, Xing C, Pertsemlidis A, Cox D, Pennacchio LA, et al. Genetic variation in PNPLA3 confers susceptibility to nonalcoholic fatty liver disease. Nat Genet 2008;40:1461-1465.
8) Kumari M, Schoiswohl G, Chitraju C, Paar M, Cornaciu I, Rangrez A, et al. Adiponutrin functions as a nutritionally regulated lysophosphatidic acid acyltransferase. Cell Metab 2012;15:691-702.
9) Lake AC, Sun Y, Li J-L, Kim JE, Johnson JW, Li D, et al. Expression, regulation, and triglyceride hydrolase activity of Adiponutrin family members. J Lipid Res 2005;46:2477-2487.
10) **Pirazzi C**, **Valenti L**, **Motta BM**, Pingitore P, Hedfalk K, Mancina RM, et al. PNPLA3 has retinyl-palmitate lipase activity in human hepatic stellate cells. Hum Mol Genet 2014;23:4077-4085.
11) Pingitore P, Pirazzi C, Mancina RM, Motta BM, Indiveri C, Pujia A, et al. Recombinant PNPLA3 protein shows triglyceride hydrolase activity and its I148M mutation results in loss of function. Biochim Biophys Acta 2014;1841:574-580.
12) Basantani MK, Sitnick MT, Cai L, Brenner DS, Gardner NP, Li JZ, et al. Pnpla3/Adiponutrin deficiency in mice does not contribute to fatty liver disease or metabolic syndrome. J Lipid Res 2011;52:318-329.
13) Baulande S, Lasnier F, Lucas M, Pairault J. Adiponutrin, a transmembrane protein corresponding to a novel dietary- and obesity-linked mRNA specifically expressed in the adipose lineage. J Biol Chem 2001;276:33336-33344.
14) Huang Y, He S, Li JZ, Seo Y-K, Osborne TF, Cohen JC, et al. A feed-forward loop amplifies nutritional regulation of PNPLA3. Proc Natl Acad Sci U S A 2010;107:7892-7897.
15) **Kilpinen H**, **Goncalves A**, Leha A, Afzal V, Alasoo K, Ashford S, et al. Common genetic variation drives molecular heterogeneity in human iPSCs. Nature 2017;546:370-375.
16) **Yusa K**, **Rashid ST**, Strick-Marchand H, Varela I, Liu PQ, Paschon DE, et al. Targeted gene correction of alpha1-antitrypsin deficiency in induced pluripotent stem cells. Nature 2011;478:391-394.
17) Hannan NRF, Segeritz C-P, Touboul T, Vallier L. Production of hepatocyte-like cells from human pluripotent stem cells. Nat Protoc 2013;8:430-437.
18) Rashid ST, Corbineau S, Hannan N, Marciniak SJ, Miranda E, Alexander G, et al. Modeling inherited metabolic disorders of the liver using human induced pluripotent stem cells. J Clin Invest 2010;120:3127-3136.
19) **Segeritz CP**, **Rashid ST**, de Brito MC, Serra MP, Ordonez A, Morell CM, et al. hiPSC hepatocyte model demonstrates the role of unfolded protein response and inflammatory networks in alpha1-antitrypsin deficiency. J Hepatol 2018;69:851-860.
20) Ortmann D, Vallier L. Variability of human pluripotent stem cell lines. Curr Opin Genet Dev 2017;46:179-185.
21) **Liu W**, **Anstee QM**, Wang X, Gawrieh S, Gamazon ER, Athinarayanan S, et al. Transcriptional regulation of PNPLA3 and its impact on susceptibility to nonalcoholic fatty liver disease (NAFLD) in humans. Aging (Albany NY) 2016;9:26-40.
22) Cohen JC, Horton JD, Hobbs HH. Human fatty liver disease: old questions and new insights. Science 2011;332:1519-1523.
23) Mota M, Banini BA, Cazanave SC, Sanyal AJ. Molecular mechanisms of lipotoxicity and glucotoxicity in nonalcoholic fatty liver disease. Metabolism 2016;65:1049-1061.
24) Eyster KM. The membrane and lipids as integral participants in signal transduction: lipid signal transduction for the non-lipid biochemist. Adv Physiol Educ 2007;31:5-16.
25) Hyysalo J, Gopalacharyulu P, Bian H, Hyotylainen T, Leivonen M, Jaser N, et al. Circulating triacylglycerol signatures in nonalcoholic fatty liver disease associated with the I148M variant in PNPLA3 and with obesity. Diabetes 2014;63:312-322.
26) **Luukkonen PK**, **Nick A**, Hölttä-Vuori M, Thiele C, Isokuortti E, Lallukka-Brück S, et al. Human PNPLA3-I148M variant increases hepatic retention of polyunsaturated fatty acids. JCI Insight 2019;4:e127902.
27) Baselli GA, Dongiovanni P, Rametta R, Meroni M, Pelusi S, Maggioni M, et al. Liver transcriptomics highlights interleukin-32 as novel NAFLD-related cytokine and candidate biomarker. Gut 2020;69:1855-1866.
28) Listenberger LL, Han X, Lewis SE, Cases S, Farese RV, Ory DS, et al. Triglyceride accumulation protects against fatty acid-induced lipotoxicity. Proc Natl Acad Sci U S A 2003;100:3077-3082.
29) Trépo E, Gustot T, Degré D, Lemmers A, Verset L, Demetter P, et al. Common polymorphism in the PNPLA3/adiponutrin gene confers higher risk of cirrhosis and liver damage in alcoholic liver disease. J Hepatol 2011;55:906-912.
30) Liu Y, Fernandez CA, Smith C, Yang W, Cheng C, Panetta JC, et al. Genome-wide study links PNPLA3 variant with elevated hepatic transaminase after acute lymphoblastic leukemia therapy. Clin Pharmacol Ther 2017;102:131-140.
31) Pastorino JG, Shulga N, Hoek JB. TNF-alpha-induced cell death in ethanol-exposed cells depends on p38 MAPK signaling but is independent of Bid and caspase-8. Am J Physiol Gastrointest Liver Physiol 2003;285:G503-G516.
32) Chung J, Chavez PRG, Russell RM, Wang X-D. Retinoic acid inhibits hepatic Jun N-terminal kinase-dependent signaling pathway in ethanol-fed rats. Oncogene 2002;21:1539-1547.
33) Trepo E, Valenti L. Update on NAFLD genetics: from new variants to the clinic. J Hepatol 2020;72:1196-1209.
34) Li JZ, Huang Y, Karaman R, Ivanova PT, Brown HA, Roddy T, et al. Chronic overexpression of PNPLA3I148M in mouse liver causes hepatic steatosis. J Clin Invest 2012;122:4130-4144.
35) He S, McPhaul C, Li JZ, Garuti R, Kinch L, Grishin NV, et al. A sequence variation (I148M) in PNPLA3 associated with nonalcoholic fatty liver disease disrupts triglyceride hydrolysis. J Biol Chem 2010;285:6706-6715.
36) Ipsen DH, Lykkesfeldt J, Tveden-Nyborg P. Molecular mechanisms of hepatic lipid accumulation in non-alcoholic fatty liver disease. Cell Mol Life Sci 2018;75:3313-3327.
37) Malhi H, Gores GJ. Molecular mechanisms of lipotoxicity in nonalcoholic fatty liver disease. Semin Liver Dis 2008;28:360-369.
38) Song MJ, Malhi H. The unfolded protein response and hepatic lipid metabolism in non alcoholic fatty liver disease. Pharmacol Ther 2019;203:107401.
39) **Luukkonen PK**, **Zhou Y**, Sädevirta S, Leivonen M, Arola J, Orešič M, et al. Hepatic ceramides dissociate steatosis and insulin resistance in patients with non-alcoholic fatty liver disease. J Hepatol 2016;64:1167-1175.

40) Mancina RM, Matikainen N, Maglio C, Söderlund S, Lundbom N, Hakkarainen A, et al. Paradoxical dissociation between hepatic fat content and de novo lipogenesis due to PNPLA3 sequence variant. J Clin Endocrinol Metab 2015;100:E821-E825.
41) Valenti L, Maggioni P, Piperno A, Rametta R, Pelucchi S, Mariani R, et al. Patatin-like phospholipase domain containing-3 gene I148M polymorphism, steatosis, and liver damage in hereditary hemochromatosis. World J Gastroenterol 2012;18:2813-2820.
42) Bruschi FV, Claudel T, Tardelli M, Caligiuri A, Stulnig TM, Marra F, et al. The PNPLA3 I148M variant modulates the fibrogenic phenotype of human hepatic stellate cells. Hepatology 2017;65:1875-1890.
43) Bruschi FV, Claudel T, Tardelli M, Starlinger P, Marra F, Trauner M. PNPLA3 I148M variant impairs liver X receptor signaling and cholesterol homeostasis in human hepatic stellate cells. Hepatol Commun 2019;3:1191-1204.
44) Pingitore P, Dongiovanni P, Motta BM, Meroni M, Lepore SM, Mancina RM, et al. PNPLA3 overexpression results in reduction of proteins predisposing to fibrosis. Hum Mol Genet 2016;25:5212-5222.
45) **Rotman Y**, **Koh C**, Zmuda JM, Kleiner DE, Liang TJ. The association of genetic variability in patatin-like phospholipase domain-containing protein 3 (PNPLA3) with histological severity of nonalcoholic fatty liver disease. Hepatology 2010;52:894-903.
46) **Krawczyk M**, **Grünhage F**, Zimmer V, Lammert F. Variant adiponutrin (PNPLA3) represents a common fibrosis risk gene: non-invasive elastography-based study in chronic liver disease. J Hepatol 2011;55:299-306.

Author names in bold designate shared co-first authorship.

Supporting Information

Additional Supporting Information may be found at onlinelibrary.wiley.com/doi/10.1002/hep.32063/suppinfo.